Exploring the Complex World of Two-Dimensional Ordering with Three Modes

S. K. Mkhonta,[1,2] K. R. Elder,[3] and Zhi-Feng Huang[1]

[1]*Department of Physics and Astronomy, Wayne State University, Detroit, Michigan 48201, USA*
[2]*Department of Physics, University of Swaziland, Private Bag 4, Kwaluseni M201, Swaziland*
[3]*Department of Physics, Oakland University, Rochester, Michigan 48309, USA*

(Received 27 May 2013; published 16 July 2013)

The world of two-dimensional crystals is of great significance for the design and study of structural and functional materials with novel properties. Here we examine the mechanisms governing the formation and dynamics of these crystalline or polycrystalline states and their elastic and plastic properties by constructing a generic multimode phase field crystal model. Our results demonstrate that a system with three competing length scales can order into all five Bravais lattices, and other more complex structures including honeycomb, kagome, and other hybrid phases. In addition, nonequilibrium phase transitions are examined to illustrate the complex phase behavior described by the model. This model provides a systematic path to predict the influence of lattice symmetry on both the structure and dynamics of crystalline and defected systems.

DOI: 10.1103/PhysRevLett.111.035501 PACS numbers: 81.10.Aj, 61.50.Ah, 81.16.Dn

Two-dimensional (2D) crystalline materials have been of tremendous interest in both fundamental research and technological applications due to their extraordinary properties and functionalities that are absent in three-dimensional materials. A typical and well-known example is graphene, which exhibits exceptional electronic, mechanical, and thermal properties [1,2]. Recent efforts have been extended to the search for and study of 2D monolayer sheets of graphene type or beyond, such as group IV elements of silicene [3] and germanane [4], BN and BNC [5], and semiconducting MoS_2 and $MoSe_2$ [6]. On larger length scales much progress has been made in the self-assembly of 2D crystals using particles of nano or micron size that are easier to tailor for specific functionalities and to observe. Colloidal crystals, for example, play a vital role in the study of structural properties of crystalline systems and the development of engineered, functional materials [7–9]. In addition, another novel technique for artificial lattice ordering is built on the trapping of ultracold atoms (e.g., ^{87}Rb) in optical superlattices produced by overlaying laser beams [10,11], as utilized for the study of many-body quantum physics.

These 2D systems involve a wide variety of constituent particles with very different types of microscopic interactions, but exhibit similar crystalline symmetries such as honeycomb (as for graphene [1], silicene [3], colloidal crystal [7], and lattices of ultracold atoms [10]), kagome (as realized for colloids [8] and ultracold ^{87}Rb [11]), and simple Bravais lattices such as triangular and square lattices [7,11]. Thus it is of fundamental importance to identify the universal mechanisms underlying these distinct modes of crystallization, based on the general principle of symmetry [12]. It is also important to understand the nature of topological defects which occur frequently in such systems and are known to determine the electronic and mechanical properties of the sample [2]. Unfortunately it is very difficult to model and predict the nature of such defected states, due to the multiple length and time scales involved in the nonequilibrium crystallization processes.

In this work we develop a dynamic model that can be applied to the study of crystallization with a variety of ordered and defected structures. We adopt the phase field crystal (PFC) formalism [13–16], in the spirit of the Alexander-McTague analysis of crystallization based on the Landau theory [12]. The advantage of this PFC approach is that one can study polycrystal formation in terms of the atomic number density on diffusive time scales that are many orders of magnitude larger than that of classical microscopic models such as molecular dynamics. One can also apply renormalization techniques [17–19] on the PFC equation to study problems that involve both micro and meso scales such as epitaxial growth [20] and surface patterning in ultrathin films [21].

Recently a great deal of progress has been made on generalizing the PFC formulation to include more crystal symmetries [22–25], although in two dimensions current PFC studies are restricted to triangular and square states. The basic idea is to incorporate interparticle interactions through a two-point direct correlation function that (i) has N peaks in Fourier space (corresponding to N different characteristic length scales) and (ii) is isotropic. This allows one to systematically interpolate between different crystalline states without *a priori* assumptions about any orientation-dependent interactions and thus allows the study of polycrystalline materials. Here we exploit this idea and show that systems with three modes (i.e., $N = 3$) exhibit a surprisingly rich phase behavior of crystallization that covers symmetries of all five 2D Bravais lattices. Our results add to a growing list of structures that can be realized from the freezing of monatomic fluids with isotropic multiwell

interaction potentials [26–29], and more importantly, provide a systematic approach for examining both structural and dynamic properties of 2D crystalline materials.

The multimode phase field crystal model we introduce here is based on a dimensionless free energy functional

$$\mathcal{F} = \int d\vec{r}\left\{\frac{\psi}{2}\left(r + \lambda \prod_{i=0}^{N-1}[(Q_i^2 + \nabla^2)^2 + b_i]\right)\psi - \frac{\tau}{3}\psi^3 + \frac{\psi^4}{4}\right\}, \quad (1)$$

as generalized from the two-mode form proposed before [24,30], and a dynamic equation $\partial\psi/\partial t = \nabla^2 \delta\mathcal{F}/\delta\psi$ on diffusive time scales, giving

$$\partial\psi/\partial t = \nabla^2\left\{\left(r + \lambda \prod_{i=0}^{N-1}[(Q_i^2 + \nabla^2)^2 + b_i]\right)\psi - \tau\psi^2 + \psi^3\right\}, \quad (2)$$

where $\psi(\vec{r}, t)$ is a rescaled particle number density field, and r, λ, b_i, and τ are phenomenological constants. The parameters b_i control the relative stability of different modes, and are determined by the interparticle potential of a specific system. This PFC free energy functional can be approximately derived from a Landau-Brazovskii expansion of the free energy in the classical density functional theory of freezing [14,18], and the gradient terms in Eq. (1) can be obtained from expanding the Fourier component of the pair correlation function in the classical density functional theory, which satisfies the requirements (i) and (ii) given above, up to its N peaks that are located at wave numbers Q_i ($i = 0, 1, \ldots, N-1$).

In a crystalline state ψ can be expanded in terms of its Fourier components $A_{\vec{q}}$ and the reciprocal lattice vectors (RLVs) $\vec{q}$: $\psi(\vec{r}) = \psi_0 + \sum_{\vec{q}} A_{\vec{q}} e^{i\vec{q}\cdot\vec{r}}$, where ψ_0 is the average rescaled density. In two dimensions, $\vec{q} = n\vec{k}_1 + m\vec{k}_2$ where m and n are integers, and $\vec{k}_1$ and $\vec{k}_2$ are the principal RLVs. From Eq. (1) we can obtain a standard expansion form

$$\mathcal{F}/V = \sum_{\vec{q}} G_{\vec{q}} A_{\vec{q}} A_{-\vec{q}} - w \sum_{\vec{q}_1\vec{q}_2\vec{q}_3} A_{\vec{q}_1} A_{\vec{q}_2} A_{\vec{q}_3} \delta_{\vec{q}_1+\vec{q}_2+\vec{q}_3,0} + \frac{1}{4} \sum_{\vec{q}_1\vec{q}_2\vec{q}_3\vec{q}_4} A_{\vec{q}_1} A_{\vec{q}_2} A_{\vec{q}_3} A_{\vec{q}_4} \delta_{\vec{q}_1+\vec{q}_2+\vec{q}_3+\vec{q}_4,0}, \quad (3)$$

where V is the system volume, $w = \tau/3 - \psi_0$, and

$$G_{\vec{q}} = \frac{1}{2}\left\{r + \lambda \prod_{i=0}^{N-1}[(Q_i^2 - q^2)^2 + b_i]\right\} - \tau\psi_0 + \frac{3}{2}\psi_0^2. \quad (4)$$

When $G_{\vec{q}}$ is small but negative, a crystalline state forms and the summation over cubic and quartic terms can be restricted to wave vectors with magnitude $|\vec{q}| = Q_i$, with higher order harmonics not needed. It was noted by Alexander and McTague [12] that close to the melting point the favored crystalline state is determined by the largest contribution of the cubic term which, according to Eq. (3), is given by a triplet of density waves with wave vectors forming a closed loop, i.e., $\vec{q}_1 + \vec{q}_2 + \vec{q}_3 = 0$.

Within the five 2D Bravais lattices the least symmetric one is oblique, a chiral lattice, for which the triplet of the density waves must consist of wave vectors with different magnitudes forming a scalene triangular loop. Thus it is a candidate of the preferred state for Eq. (3) when $N = 3$. The same argument holds for the rectangular lattice. The square or rhombic lattice can be considered as special cases of the rectangular or oblique lattice that is stabilized with $N = 2$ and with triads of wave vectors forming an isosceles triangular loop. This $N = 2$ limit was explored by Lifshitz and Petrich [30], showing stable patterns of two-, four-, six-, and 12-fold symmetries. The $N = 1$ limit, with the basic wave vectors forming an equilateral triangle, corresponds to the favored 2D triangular phase as given in the classical work of Alexander and McTague [12]. Thus three modes (with different Q_i, $i = 0, 1, 2$) are enough for constructing a minimal model to cover all five 2D Bravais lattices. Furthermore, the selection and competition between these modes of different length scales will lead to much richer crystalline phases, an effect that goes beyond the classical Alexander-McTague type analysis. As shown below, we can tune the excitation level of the density waves of $|\vec{q}| = Q_i$ via parameters b_i in our PFC model to systematically explore the stability of different phases that compete with a targeted crystalline state.

To verify our analysis we solved the PFC dynamic equation (2) with $N = 3$ via a pseudospectral algorithm [31,32], using periodic boundary conditions in systems of sizes ranging from 256^2 to 1024^2. We restricted our parameter space to $\psi_0 = -0.2$, $r = -0.15$, $\lambda = 0.02$, and $\tau = 0$ for simplicity. To systematically determine the various steady states we chose Q_i such that the magnitudes of the critical wave vectors correspond to the three shortest wave numbers of a targeted lattice. For a 2D Bravais lattice they are given by

$$|\vec{q}| = k_1\sqrt{m^2 + \mu^2 n^2 + 2mn\mu\cos\theta}, \quad (5)$$

where $\mu = k_2/k_1$ and θ is the angle between $\vec{k}_1$ and $\vec{k}_2$.

Steady-state solutions were obtained by monitoring the crystallization process until changes in the system free energy density are negligible (e.g., $\Delta f < 0.01\%$). In Fig. 1 we show a variety of ordered states obtained when $Q_{i=0,1,2} = 1, \sqrt{3}, 2$ (corresponding to the first three shortest RLVs for the triangular lattice), at different regions of the b_i parameter space. They include three triangular (Tri0, Tri1, Tri2), honeycomb (Hon), kagome (Kag), rectangular (Rec), dimer (Dim), and intermediate (Int) phases. We identified the observed regions of these different states by rerunning the simulations (using different random initial conditions) at each point of the parameter space for more than 10 times and classifying the stable structure as the equilibrium phase. The results are depicted in Fig. 2.

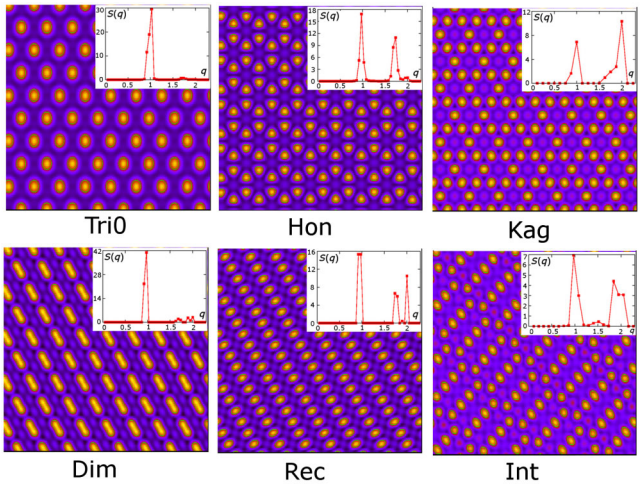

FIG. 1 (color online). Crystalline phases obtained via PFC simulations for $Q_{i=0,1,2} = 1,\ \sqrt{3},\ 2$, including one of three triangular phases (Tri0), kagome (Kag), honeycomb (Hon), dimer (Dim), and rectangular (Rec) phases, and also an intermediate phase (Int). Insets: the circularly averaged structure factor $S(q)$ vs q.

These simulation results are consistent with the above crystallization analysis. The stable triangular states are characterized by a circularly averaged structure factor $S(q)$ with one dominant peak, as shown in Fig. 1. The honeycomb phase corresponds to a superposition of two sets of triplet density waves with $|\vec{q}| = Q_0$ and Q_1, respectively. Each set can maximize the cubic free energy term since the wave vectors can form a closed loop (equilateral triangle). Similar arguments can be made for the kagome phase, but with each set having wave vectors $|\vec{q}| = Q_0$ and Q_2, respectively. This has been demonstrated in the experiments of ultracold atoms [11], where two sets of three optical waves with $|\vec{q}| = Q_0$ and $Q_2 = 2Q_0$ were superimposed to create a kagome lattice. To further examine the formation condition of the honeycomb phase we analyze the following transformation: Tri1 → Hon → Dim. The Tri1 → Hon transformation is characterized by a sudden increase of the structure-factor peak at Q_0, leading to two prominent peaks in the honeycomb phase [see Fig. 3(a)]. A further increase in b_1 creates an imbalance between the two sets of critical modes, inducing a compressed-honeycomb, i.e., dimer, state. Figure 3 shows the dynamics of the Hon → Dim transformation. A pair of density maxima merge to form elongated regions of higher densities (i.e., dimers) during the transition.

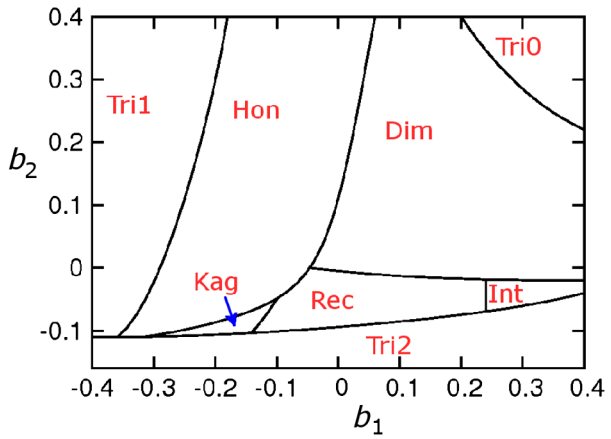

FIG. 2 (color online). Phases determined from the PFC model with $Q_{i=0,1,2} = 1,\ \sqrt{3},\ 2$, and $b_0 = 0$.

As discussed above, three modes are needed to form a rectangular phase, which is verified in our results of Fig. 1. Our numerical results also reveal that one can interpolate between the two Bravais lattice symmetries triangular and rectangular by tuning the excitation levels of the dominant density waves via b_i. This is not surprising since from Eq. (5) one can see that the magnitudes of the RLVs in a triangular lattice $Q_{i=0,1,2} = 1,\ \sqrt{3},\ 2$ are the same as those of a rectangular lattice with $\mu = \sqrt{3}$. We have realized a stable intermediate state between these two lattices (see Fig. 1), which consists of rectangular domains separated periodically by triangular edges. An analogous phase has been observed in experiments involving the commensurate phase ordering of colloid monolayers (i.e., Archimedean-like tiling [9]).

We can also target the ordering into other 2D Bravais lattices: square, rhombic, and oblique, by applying Eq. (5). The ratio of the three shortest wave vectors in a square lattice is given by $Q_{i=0,1,2} = 1,\ \sqrt{2},\ 2$, leading to two possible sets of density wave triplets: two with $|\vec{q}| = 1$ and one with $|\vec{q}| = \sqrt{2}$, or two with $|\vec{q}| = \sqrt{2}$ and one with $|\vec{q}| = 2$. Both have been obtained in our simulations, with an example shown in Fig. 4(a). We also observed other stable states with the same Q_i series, including three triangular states and a phase that consists of pentagons and hexagons [see Fig. 4(b)] with dominant structure-factor

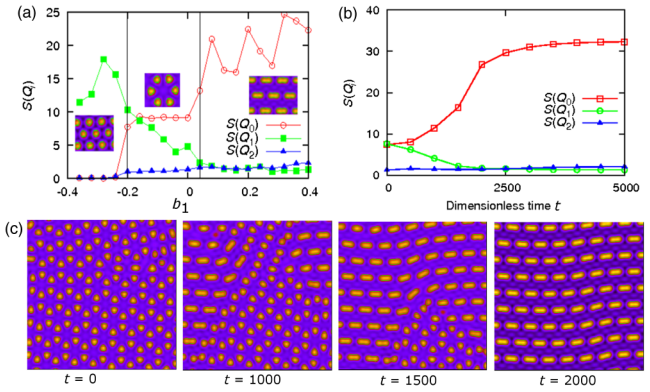

FIG. 3 (color online). Dynamic process of phase transformation. (a) Peak values of structure factor during a Tri1 → Hon → Dim transformation, for $(b_0, b_2) = (0, 0.1)$. (b),(c) Dynamics of a Hon → Dim transformation from $(b_0, b_1, b_2) = (0, -0.1, 0.04)$ to $(0, 0.2, 0.04)$.

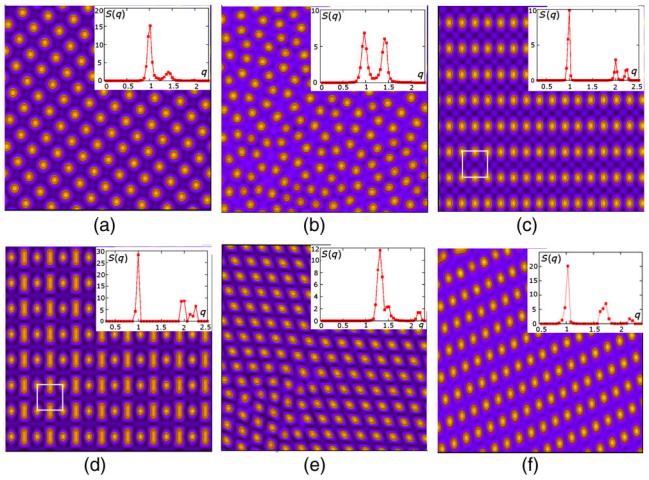

FIG. 4 (color online). (a) Square and (b) pentagon-hexagon structures are obtained with $Q_{i=0,1,2} = 1, \sqrt{2}, 2$. Example phases with $Q_{i=0,1,2} = 1, 2, \sqrt{5}$ are shown as (c) a rectangular phase and (d) a dimer-square crystal, with their square unit cells indicated. Also (e) a rhombic phase at $Q_{i=0,1,2} = 1.35, 1.57, 2.2$ and (f) an oblique phase at $Q_{i=0,1,2} = 1, \sqrt{3}, 2.2$ are given.

peaks located at $|\vec{q}| = Q_0$ and Q_1. A similar pentagon phase was found in recent molecular dynamics simulations using a double-well potential [27].

The square-type states can be also generated from the series $Q_{i=0,1,2} = 1, 2, \sqrt{5}$, although with a multiatom basis. Note that this Q_i series corresponds to a closed loop of right-angled-triangle wave vectors, and thus a rectangular state, as seen in Fig. 4(c). However, such a phase can be defined as a square lattice with a two-atom basis since this Q_i series also incorporates the ratio of the Bragg peak positions of a square structure. Another stable multiatom square state, a square-dimer phase, is shown in Fig. 4(d).

To reproduce a rhombic or oblique phase, we note that in general the oblique state is favored by the cubic term of free energy expansion when $|b_i| \ll 1$, where all the three critical modes are excited, while the rhombic phase is favored when two different modes are dominant. As shown in our results of Figs. 4(e) and 4(f), the structure factor of the oblique phase is characterized by three peaks and the rhombic phase by two dominant peaks, as expected.

Another focus of our work is on exploring the dynamics of different crystalline states that are generated by the three-mode PFC model. Starting from an unstable, homogeneous liquid state, the typical crystallization process of a large system involves the nucleation of crystal seeds, and the formation and later the annihilation of topological defects which leads to the growth and coarsening of crystal grains. In Fig. 5 we show a variety of topological defects observed during the ordering process. This includes linear and point defects in the honeycomb phase, grain boundaries in the oblique lattice, and complex defected states associated with coexistence of different crystalline structures, and also disclinations in the dimer state.

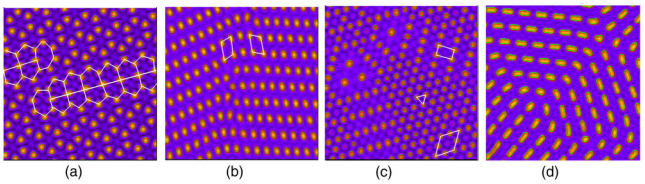

FIG. 5 (color online). Snapshots of defect configurations during dynamic simulations, for (a) honeycomb phase, (b) oblique phase, (c) coexisting phases, and (d) dimer phase.

The simplicity of our approach also makes it relatively straightforward to calculate the elastic properties of these crystalline states. As shown in Fig. 1, the structure factor of the dimer phase has a dominant single peak and thus a one-mode approximation [13,16,33] can be utilized. Note also that the dimer structure results from the merging of two density peaks in a honeycomb phase, as demonstrated in Fig. 3. Hence here we can consider $\psi(\vec{r})$ as a two-particle (dimer) density, with each constituent dimer molecule (basis) consisting of two atoms, one at the origin and the other at $(\kappa d, 0)$, where $0 < \kappa < 1/2$ and d is the lattice constant of the corresponding triangular lattice they occupy. Following the standard procedure [16], we obtain the shear modulus of the system $\mu_s = C_{44} = 3\alpha_t[\cos(2\kappa\pi) + 1]/8$ where $\alpha_t = (b_1 + 4q^4) \times (b_2 + 9q^4)\lambda A^2 q^4$, A is the amplitude of the ψ expansion, and $q = 4\pi/(\sqrt{3}d) = Q_0$, and the anisotropic Poisson ratios parallel and perpendicular to the dimer molecular axis are

$$\nu_x = \frac{C_{12}}{C_{22}} = 3\left[\frac{\cos(2\kappa\pi) + 1}{\cos(2\kappa\pi) + 17}\right] \quad \text{and} \quad \nu_y = \frac{C_{12}}{C_{11}} = \frac{1}{3}. \tag{6}$$

When $\kappa \to 0$ the dimer state changes to a triangular one (Tri0). In this limit the Poisson ratio becomes isotropic as obtained from Eq. (6), which is expected for an elastically isotropic triangular lattice. Our calculations also show that the shear modulus of the dimer state is smaller than that of the triangular phase. This is a consequence of the additional degree of freedom in this state; i.e., the dimers can rotate [33]. When $\kappa \to 1/2$, the simple one-mode approximation used here breaks down and more harmonics (modes) are required. This would correspond to the instability of the dimer phase towards the formation of the honeycomb phase (which is described by two modes) around the point of $\kappa = 1/2$.

All our results presented above show that crystallization is not only a general problem of symmetry as was first argued by Alexander and McTague three decades ago [12], but also a problem involving competition and coupling between different length scales of the system. As demonstrated, three modes are enough to produce all five Bravais lattices in two dimensions as well as many of the non-Bravais structures, including honeycomb and kagome

phases that have been found in novel 2D crystalline materials, and also predictions of more complex phases. The minimal model presented here can be exploited to study not only the nonequilibrium formation of crystals and polycrystals with a large variety of crystalline symmetries, but also the elastic and plastic properties of such systems [34–36]. Our results can also serve as a guide to experiments on producing or self-assembling a variety of ordered phases that can form in systems with competing multiple scales, such as the ordering process of surface-functionalized colloidal particles or of ultracold atoms in tunable commensurate optical lattices. The study of such a self-assembly process and the evolution of a defected state requires a dynamic modeling method at time scales of experimental relevance, for which the multimode PFC model described here is much more applicable than conventional atomistic techniques. Furthermore, our modeling framework can be readily extended to a systematic study of three-dimensional crystalline and polycrystalline materials or self-assembled systems.

We acknowledge support from the National Science Foundation under Grants No. DMR-0845264 (Z.-F. H.) and No. DMR-0906676 (K. R. E.).

[1] A. K. Geim and K. S. Novoselov, Nat. Mater. **6**, 183 (2007).
[2] S. T. Pantelides, Y. Puzyrev, L. Tsetseris, and B. Wang, MRS Bull. **37**, 1187 (2012).
[3] P. Vogt, P. De Padova, C. Quaresima, J. Avila, E. Frantzeskakis, M. C. Asensio, A. Resta, B. Ealet, and G. Le Lay, Phys. Rev. Lett. **108**, 155501 (2012).
[4] E. Bianco, S. Butler, S. Jiang, O. D. Restrepo, W. Windl, and J. E. Goldberger, ACS Nano **7**, 4414 (2013).
[5] L. Ci, L. Song, C. Jin, D. Jariwala, D. Wu, Y. Li, A. Srivastava, Z. F. Wang, K. Storr, L. Balicas, F. Liu, and P. M. Ajayan, Nat. Mater. **9**, 430 (2010).
[6] S. Tongay, J. Zhou, C. Ataca, K. Lo, T. S. Matthews, J. Li, J. C. Grossman, and J. Wu, Nano Lett. **12**, 5576 (2012).
[7] N. Osterman, D. Babic, I. Poberaj, J. Dobnikar, and P. Ziherl, Phys. Rev. Lett. **99**, 248301 (2007).
[8] Q. Chen, S. C. Bae, and S. Granick, Nature (London) **469**, 381 (2011); X. Mao, Q. Chen, and S. Granick, Nat. Mater. **12**, 217 (2013).
[9] J. Mikhael, J. Roth, L. Helden, and C. Bechinger, Nature (London) **454**, 501 (2008).
[10] P. Soltan-Panahi, J. Struck, P. Hauke, A. Bick, W. Plenkers, G. Meineke, C. Becker, P. Windpassinger, M. Lewenstein, and K. Sengstock, Nat. Phys. **7**, 434 (2011).
[11] G.-B. Jo, J. Guzman, C. K. Thomas, P. Hosur, A. Vishwanath, and D. M. Stamper-Kurn, Phys. Rev. Lett. **108**, 045305 (2012).
[12] S. Alexander and J. McTague, Phys. Rev. Lett. **41**, 702 (1978).
[13] K. R. Elder, M. Katakowski, M. Haataja, and M. Grant, Phys. Rev. Lett. **88**, 245701 (2002); K. R. Elder and M. Grant, Phys. Rev. E **70**, 051605 (2004).
[14] K. R. Elder, N. Provatas, J. Berry, P. Stefanovic, and M. Grant, Phys. Rev. B **75**, 064107 (2007).
[15] H. Emmerich, H. Löwen, R. Wittkowski, T. Gruhn, G. I. Tóth, G. Tegze, and L. Gránásy, Adv. Phys. **61**, 665 (2012).
[16] N. Provatas and K. R. Elder, *Phase Field Methods in Materials Science and Engineering* (Wiley-VCH, Weinheim, 2010).
[17] N. Goldenfeld, B. P. Athreya, and J. A. Dantzig, Phys. Rev. E **72**, 020601(R) (2005).
[18] Z.-F. Huang, K. R. Elder, and N. Provatas, Phys. Rev. E **82**, 021605 (2010).
[19] Z.-F. Huang, Phys. Rev. E **87**, 012401 (2013).
[20] Z.-F. Huang and K. R. Elder, Phys. Rev. Lett. **101**, 158701 (2008); Phys. Rev. B **81**, 165421 (2010).
[21] K. R. Elder, G. Rossi, P. Kanerva, F. Sanches, S.-C. Ying, E. Granato, C. V. Achim, and T. Ala-Nissila, Phys. Rev. Lett. **108**, 226102 (2012).
[22] A. G. Khachaturyan (private communication).
[23] M. Greenwood, N. Provatas, and J. Rottler, Phys. Rev. Lett. **105**, 045702 (2010).
[24] K.-A. Wu, A. Adland, and A. Karma, Phys. Rev. E **81**, 061601 (2010).
[25] K.-A. Wu, M. Plapp, and P. W. Voorhees, J. Phys. Condens. Matter **22**, 364102 (2010).
[26] M. C. Rechtsman, F. H. Stillinger, and S. Torquato, Phys. Rev. Lett. **95**, 228301 (2005).
[27] M. Engel and H.-R. Trebin, Phys. Rev. Lett. **98**, 225505 (2007).
[28] E. Edlund, O. Lindgren, and M. N. Jacobi, Phys. Rev. Lett. **107**, 085503 (2011); **108**, 165502 (2012).
[29] R. D. Batten, D. A. Huse, F. H. Stillinger, and S. Torquato, Soft Matter **7**, 6194 (2011).
[30] R. Lifshitz and D. M. Petrich, Phys. Rev. Lett. **79**, 1261 (1997).
[31] M. Cheng and J. A. Warren, J. Comput. Phys. **227**, 6241 (2008).
[32] X.-F. Wu and Y. A. Dzenis, Phys. Rev. E **77**, 031807 (2008).
[33] S. K. Mkhonta, D. Vernon, K. R. Elder, and M. Grant, Europhys. Lett. **101**, 56004 (2013).
[34] G. Tegze, G. I. Tóth, and L. Gránásy, Phys. Rev. Lett. **106**, 195502 (2011).
[35] J. Berry, K. R. Elder, and M. Grant, Phys. Rev. E **77**, 061506 (2008).
[36] P. Y. Chan, G. Tsekenis, J. Dantzig, K. A. Dahmen, and N. Goldenfeld, Phys. Rev. Lett. **105**, 015502 (2010).